Optical Engineering

OpticalEngineering.SPIEDigitalLibrary.org

# Method of confocal mirror design

José Sasián

SPIE.

José Sasián, "Method of confocal mirror design," *Opt. Eng.* **58**(1), 015101 (2019), doi: 10.1117/1.OE.58.1.015101.

Optical Engineering 58(1), 015101 (January 2019)

# Method of confocal mirror design

**José Sasián***
University of Arizona, College of Optical Sciences, Tucson, Arizona, United States

**Abstract.** We provide an overview of the method of confocal mirror design and report advances with respect to pupil imagery. Two real ray-based conditions, $Y^{+} = -Y^{-}$ and $\Delta Y = 0$, for the absence of linear astigmatism and field tilt are presented. One example illustrates the design of a system confocal of the object and image, and another illustrates the design of a system confocal of the pupils. Stop shifting formulas are provided. Three three-mirror anastigmatic systems further illustrate the method.  [DOI: 10.1117/1.OE.58.1.015101]

Keywords: unsymmetrical systems; freeform surfaces; pupil aberrations; confocal imaging; plane symmetry; linear astigmatism; field tilt; three-mirror anastigmatic systems.

Paper 181506 received Oct. 21, 2018; accepted for publication Dec. 6, 2018; published online Jan. 5, 2019.

## 1 Introduction

The word confocal means having a common focus or foci. The design method of confocal mirror systems, and confocal refractive systems, is very old. This method was used by Cassegrain and Mersenne in their famous telescope mirror configurations. However, little or nothing has been done to advance the confocal design method when used for axially symmetric systems. In the case of refractive systems, one advancement would be to combine lens elements where each lens element is aplanatic. Fourth-order theory shows that the astigmatism of each element does not change upon stop shifting. If all the lenses are made of the same glass then field curvature is corrected when astigmatism is corrected. An aplanatic and confocal lens concatenation is conceptually simple and useful to lay out a starting lens design.

In the case of nonaxially symmetric systems, the method of confocal design turns out to be a powerful method. One reason is that the method provides excellent starting design points. Another is that the method can be applied in a very systematic manner. Still another reason is that the surfaces required have as a base surface an off-axis conic surface, or off-axis Cartesian ovoid for refractive systems, which has two foci where it can be optically tested.

Because of the potential innovation in optical systems, nonaxially symmetric systems using freeform surfaces are enjoying attention from the optical design community. Important classes of systems are those that are reflective and have a plane of symmetry, as fabrication and alignment are feasible. The question is how to design such reflective plane symmetric systems. Although there are several approaches to design optical systems, we highlight what we call the method of confocal mirror design.[1,2] In the present context, a confocal system is defined as a mirror system that provides point images, surface after surface, along a selected ray called the optical axis ray (OAR). The field center, the center of the stop, and the pupils are centered about the OAR. As shown in Fig. 1 for a two-mirror system, point imaging along the OAR requires the surfaces to be on-axis or off-axis conic sections. Confocal systems are receiving recently some attention[3–6] as they provide useful starting design points. In this paper, we review their theory, report some advances pertaining to pupil imagery, present a real ray-based condition for the absence of linear astigmatism, discuss an ad hoc optical surface, and summarize a systematic design approach. Some design examples are provided. A reduced version of this paper has been previously published.[7]

## 2 Review of Aberrations of a Plane Symmetric System

The aberration function $W(\vec{i},\vec{H},\vec{\rho})$ for a plane symmetric system[1] can be written as

$$W(\vec{i},\vec{H},\vec{\rho}) = \sum_{k,m,n,p,q}^{\infty} W_{\substack{2k+n+p,\\2m+n+q,\\n,p,q}} (\vec{H}\cdot\vec{H})^{k}(\vec{\rho}\cdot\vec{\rho})^{m}(\vec{H}\cdot\vec{\rho})^{n}(\vec{i}\cdot\vec{H})^{p}(\vec{i}\cdot\vec{\rho})^{q},$$

where $W_{2k+n+p,2m+n+q,n,p,q}$ is the coefficient of a particular aberration form defined by the integers $k$, $m$, $n$, $p$, and $q$. The lower indices in the coefficients indicate the algebraic powers of $H$, $\rho$, $\cos(\phi)$, $\cos(\chi)$, and $\cos(\chi+\phi)$ in a given aberration term. The angle $\chi$ is between the vectors $\vec{i}$ and $\vec{H}$, and the angle $\chi+\phi$ is between the vectors $\vec{i}$ and $\vec{\rho}$. By setting the sum of the integers to 0, 1, 2,..., groups of aberrations are defined as shown in Table 3. The vector $\vec{i}$ defines the direction of plane symmetry, $\vec{\rho}$ is the aperture vector at the exit pupil, and $\vec{H}$ is the field vector at the object plane. A ray in the system is uniquely defined by $\vec{H}$ and $\vec{\rho}$, and the aberration function provides the optical path for every ray.

A study of Table 1 provides useful insights. The aberration terms are divided into groups and in turn in subgroups according to symmetry characteristics. Thus, the third group contains the primary aberrations of axially symmetric systems as a subgroup, contains the aberrations of double-plane symmetric systems as a subgroup, and a subgroup of aberrations for plane symmetric systems that are not

*Address all correspondence to José Sasián, E-mail: jose.sasian@optics.arizona.edu

0091-3286/2019/$25.00 © 2019 SPIE

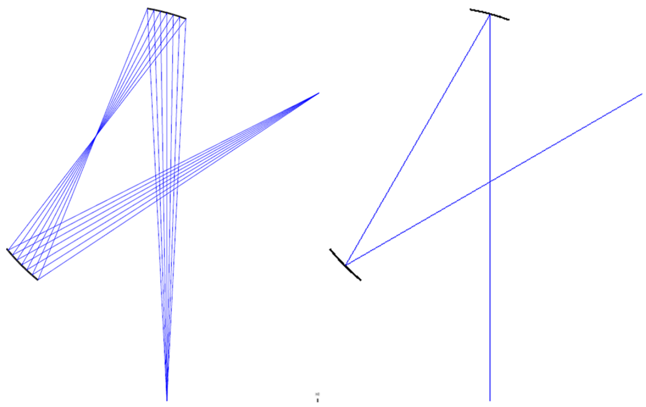


**Fig. 1** (a) A two mirror confocal system consisting of two off-axis elliptical mirrors. (b) The central ray is the OAR.

**Table 1** Aberration terms of a plane symmetric system.

| | |
|---|---|
| First group | |
| $W_{00000}$ | Piston |
| Second group | |
| $W_{01001}\vec{i}\cdot\vec{\rho}$ | Field displacement |
| $W_{10010}\vec{i}\cdot\vec{H}$ | Linear piston |
| $W_{02000}\vec{\rho}\cdot\vec{\rho}$ | Defocus |
| $W_{11100}\vec{H}\cdot\vec{\rho}$ | Magnification |
| $W_{20000}\vec{H}\cdot\vec{H}$ | Quadratic piston |
| Third group | |
| $W_{02002}(\vec{i}\cdot\vec{\rho})^2$ | Uniform astigmatism |
| $W_{11011}(\vec{i}\cdot\vec{H})(\vec{i}\cdot\vec{\rho})$ | Anamorphic distortion |
| $W_{20020}(\vec{i}\cdot\vec{H})^2$ | Quadratic piston |
| $W_{03001}(\vec{i}\cdot\vec{\rho})(\vec{\rho}\cdot\vec{\rho})$ | Uniform coma |
| $W_{12101}(\vec{i}\cdot\vec{\rho})(\vec{H}\cdot\vec{\rho})$ | Linear astigmatism |
| $W_{12010}(\vec{i}\cdot\vec{H})(\vec{\rho}\cdot\vec{\rho})$ | Field tilt |
| $W_{21001}(\vec{i}\cdot\vec{\rho})(\vec{H}\cdot\vec{H})$ | Quadratic distortion I |
| $W_{21110}(\vec{i}\cdot\vec{H})(\vec{H}\cdot\vec{\rho})$ | Quadratic distortion II |
| $W_{30010}(\vec{i}\cdot\vec{H})(\vec{H}\cdot\vec{H})$ | Cubic piston |
| $W_{04000}(\vec{\rho}\cdot\vec{\rho})^2$ | Spherical aberration |
| $W_{13100}(\vec{H}\cdot\vec{\rho})(\vec{\rho}\cdot\vec{\rho})$ | Linear coma |
| $W_{22200}(\vec{H}\cdot\vec{\rho})^2$ | Quadratic astigmatism |
| $W_{22000}(\vec{H}\cdot\vec{H})(\vec{\rho}\cdot\vec{\rho})$ | Field curvature |
| $W_{31100}(\vec{H}\cdot\vec{H})(\vec{H}\cdot\vec{\rho})$ | Cubic distortion |
| $W_{40000}(\vec{H}\cdot\vec{H})^2$ | Quartic piston |

axially or double-plane symmetric. Thus, the aberration properties of a plane symmetric system can be thought of as the superposition of the properties of axial, double plane, and plane symmetric systems. The correction of the aberrations of a given subgroup can be carried out using system properties according to subgroup symmetry. For example, using a freeform surface having axial $Z_\alpha$, double plane $Z_\beta$, or plane symmetry $Z_\gamma$. Mathematically, these aspheric terms are

$$Z_\alpha = \alpha(\vec{\rho}\cdot\vec{\rho})^2,$$

$$Z_\beta = \beta(\vec{i}\cdot\vec{\rho})^2,$$

$$Z_\gamma = \gamma(\vec{i}\cdot\vec{\rho})(\vec{\rho}\cdot\vec{\rho}),$$

where $\alpha$, $\beta$, and $\gamma$ are the aspheric coefficients.

The coefficients of the first and second groups in Table 1 are set to zero because piston terms do not degrade the image, and second-order optics predicts the image size and location.

Because Table 1 has as subgroups the aberrations of axially symmetric systems, double-plane symmetric systems, and plane symmetric systems, we can treat a plane symmetric system as the superposition of three systems according to symmetry. In particular, we can associate an axially symmetric system to a plane symmetric system. Then, the second-order properties of the plane symmetric system are given by the second-order properties of the associated axially symmetric system. Using the oblique power

$$\phi_{\text{oblique}} = \frac{2\cos(I)}{r_s},$$

for each surface in the system, we then can use any of the standard methods for axially symmetric systems to calculate second-order properties of the plane symmetric system. For example, the focal lengths, and the image position and size. In the oblique power, $I$ is the angle of incidence of the OAR in the surface and $r_s$ is the sagittal radius of the surface at the OAR intersection. In what follows, we will not discuss the subgroup of aberrations that belong to axially symmetric systems as these are well understood. These aberrations depend only on the rotational invariants $(\vec{H}\cdot\vec{H})$, $(\vec{H}\cdot\vec{\rho})$, and $(\vec{\rho}\cdot\vec{\rho})$.

For the case of a confocal reflective system that is plane symmetric,[1] some of the coefficients in the third group are zero as shown in Table 2. Field tilt is proportional to linear astigmatism, and provided there is enough surface optical power, one surface tilt can be used to correct for both linear astigmatism and field tilt simultaneously. Furthermore, the coefficient for quadratic distortion II is zero. Except for quadratic distortion I, if left uncorrected, a confocal system may act as an axially symmetric system to the fourth-order of approximation. Thus, a confocal reflective system provides an excellent starting design point.

In a similar manner to the derivation of the image aberration function, and since the entrance and exit pupils are optically conjugated, we can derive a pupil aberration function $\bar{W}(\vec{i},\vec{H},\vec{\rho})$ for a plane symmetric system and write it to fourth-order as

**Table 2** Aberration coefficients a plane symmetric system that is confocal of the image.

| Third group | |
|---|---|
| $W_{02002} = 0$ | Uniform astigmatism |
| $W_{11011} = 0$ | Anamorphic distortion |
| $W_{20020} = 0$ | Quadratic piston |
| $W_{03001} = 0$ | Uniform coma |
| $W_{12101}$ | Linear astigmatism |
| $W_{12010} = -\frac{1}{2} W_{12101}$ | Field tilt |
| $W_{21001}$ | Quadratic distortion I (smile) |
| $W_{21110} = 0$ | Quadratic distortion II (keystone) |
| $W_{30010}$ | Cubic piston |

**Table 4** Aberration coefficients of a plane symmetric system that is confocal of the pupils.

| Third group | |
|---|---|
| $\overline{W}_{02002} = 0$ | Pupil uniform astigmatism |
| $\overline{W}_{11011} = 0$ | Pupil anamorphic distortion |
| $\bar{W}_{20020} = 0$ | Pupil quadratic piston |
| $\overline{W}_{03001} = 0$ | Pupil uniform coma |
| $\overline{W}_{12101}$ | Pupil linear astigmatism |
| $\overline{W}_{12010} = -\frac{1}{2} \overline{W}_{12101}$ | Pupil field tilt |
| $\overline{W}_{21001}$ | Pupil quadratic distortion I |
| $\overline{W}_{21110} = 0$ | Pupil quadratic distortion II |
| $\overline{W}_{30010}$ | Pupil cubic piston |

$$\begin{aligned}\overline{W}(\vec{i},\vec{H},\vec{\rho}) &= \overline{W}_{00000} \\ &+ \overline{W}_{02002}(\vec{i}\cdot\vec{H})^2 + \overline{W}_{11011}(\vec{i}\cdot\vec{H})(\vec{i}\cdot\vec{\rho}) + \overline{W}_{20020}(\vec{i}\cdot\vec{\rho})^2 \\ &+ \overline{W}_{02000}(\vec{H}\cdot\vec{H}) + \overline{W}_{11100}(\vec{H}\cdot\vec{\rho}) + \overline{W}_{20000}(\vec{\rho}\cdot\vec{\rho}) \\ &+ \overline{W}_{03001}(\vec{i}\cdot\vec{H})(\vec{H}\cdot\vec{H}) + \overline{W}_{12101}(\vec{i}\cdot\vec{H})(\vec{H}\cdot\vec{\rho}) \\ &+ \overline{W}_{12010}(\vec{i}\cdot\vec{\rho})(\vec{H}\cdot\vec{H}) + \overline{W}_{21001}(\vec{i}\cdot\vec{H})(\vec{\rho}\cdot\vec{\rho}) \\ &+ \overline{W}_{21110}(\vec{i}\cdot\vec{\rho})(\vec{H}\cdot\vec{\rho}) + \overline{W}_{30010}(\vec{i}\cdot\vec{\rho})(\vec{\rho}\cdot\vec{\rho}) \\ &+ \overline{W}_{04000}(\vec{H}\cdot\vec{H})^2 + \overline{W}_{13100}(\vec{H}\cdot\vec{H})(\vec{H}\cdot\vec{\rho}) \\ &+ \overline{W}_{22200}(\vec{H}\cdot\vec{\rho})^2 + \overline{W}_{22000}(\vec{H}\cdot\vec{H})(\vec{\rho}\cdot\vec{\rho}) \\ &+ \overline{W}_{31100}(\vec{H}\cdot\vec{\rho})(\vec{\rho}\cdot\vec{\rho}) + \overline{W}_{40000}(\vec{\rho}\cdot\vec{\rho})^2.\end{aligned}$$

## 3 Relationships between Pupil and Image Aberration Coefficients in Confocal Systems

It turns out[8,9] that for a reflective plane symmetric system, the image and pupil aberration coefficients of fourth-order on $\vec{i}$, $\vec{\rho}$, and $\vec{H}$ are connected by the identities in Table 3. For these identities to hold, it is required that no surface with optical power in the system coincides with the stop aperture or the pupils.

In addition, we can rewrite Table 2 for the pupil imagery as shown in Table 4.

Then using the identities in Tables 3 and 4, we can write the aberration coefficients of the image when the system is confocal of the pupils as shown in Table 5.

The relationships in Table 5 provide new insights about confocal systems. Specifically, the image aberrations of a plane symmetric system that is confocal of the pupils are as follows. There is no quadratic piston, anamorphic distortion, or uniform astigmatism. These three aberrations depend on the double-plane symmetric invariants $(\vec{i}\cdot\vec{H})^2$, $(\vec{i}\cdot\vec{\rho})^2$, and $(\vec{i}\cdot\vec{H})(\vec{i}\cdot\vec{\rho})$. There is no cubic piston of the image and the quadratic distortions are linked; if one is zero the other is zero too. There is no linear astigmatism either or quadratic astigmatism. Uniform coma can be present and can be corrected with a comatic like freeform asphericity

**Table 3** Pupil and image aberration coefficient equalities for a reflective plane symmetric system.

| Pupil aberration | Coefficient equality | Image aberration |
|---|---|---|
| Pupil uniform astigmatism | $\overline{W}_{02002} = W_{20020}$ | Quadratic piston |
| Pupil anamorphic distortion | $\overline{W}_{11011} = W_{11011}$ | Anamorphic distortion |
| Pupil quadratic piston | $\overline{W}_{20020} = W_{02002}$ | Uniform astigmatism |
| Pupil uniform coma | $\overline{W}_{03001} = W_{30010}$ | Cubic piston |
| Pupil linear astigmatism | $\overline{W}_{12101} = W_{21110}$ | Quadratic distortion II |
| Pupil field tilt | $\overline{W}_{12010} = W_{21001}$ | Quadratic distortion I |
| Pupil quadratic distortion I | $\overline{W}_{21001} = W_{12010}$ | Field tilt |
| Pupil quadratic distortion II | $\overline{W}_{21110} = W_{12101}$ | Linear astigmatism |
| Pupil cubic piston | $\overline{W}_{30010} = W_{03001}$ | Uniform coma |

**Table 5** Image aberration coefficients of a plane symmetric system that is confocal of the pupils.

| Image aberration | Coefficient equality | Pupil aberration |
|---|---|---|
| Quadratic piston | $W_{20020} = \overline{W}_{02002} = 0$ | Pupil uniform astigmatism |
| Anamorphic distortion | $W_{11011} = \overline{W}_{11011} = 0$ | Pupil anamorphic distortion |
| Uniform astigmatism | $W_{02002} = \overline{W}_{20020} = 0$ | Pupil quadratic piston |
| Cubic piston | $W_{30010} = \overline{W}_{03001} = 0$ | Pupil uniform coma |
| Quadratic distortion II | $W_{21110} = \overline{W}_{12101}$ | Pupil linear astigmatism |
| Quadratic distortion I | $W_{21001} = -\frac{1}{2} W_{21110} = \overline{W}_{12010} = -\frac{1}{2} \overline{W}_{12101}$ | Pupil field tilt |
| Field tilt | $W_{12010} = \overline{W}_{21001}$ | Pupil quadratic distortion I |
| Linear astigmatism | $W_{12101} = \overline{W}_{21110} = 0$ | Pupil quadratic distortion II |
| Uniform coma | $W_{03001} = \overline{W}_{30010}$ | Pupil cubic piston |

$Z_\gamma = \gamma(\vec{i} \cdot \vec{\rho})(\vec{\rho} \cdot \vec{\rho})$ at a surface coinciding with a pupil or the stop aperture. Field tilt can be present.

Clearly, there are two approaches to start the design of a plane symmetric system. The first approach is to lay out a system that is confocal of the image, the second approach is to lay out a system that is confocal of the pupils.

## 4 Stop Shifting Formulas

As we have the requirement of not having a surface at the stop, or pupils, we present stop shifting formulas to gain insights about how the aberrations change as we shift the stop. Stop shifting may be necessary after a preliminary design. Stop shifting is carried out by substituting the vector $\vec{\rho} + S\vec{H}$ in place of $\vec{\rho}$ in any aberration terms in the system. Table 6 shows the new aberration coefficients marked with an asterisk when there is aberration present and stop shifting is performed. Stop shifting is quantified by the parameter $\overline{S}$, which depends on the marginal and chief ray heights at any surface in the associated axially symmetric system and given as

$$\overline{S} = \frac{\overline{y}_{\mathrm{new}} - \overline{y}_{\mathrm{old}}}{y}.$$

## 5 AD-HOC Freeform Surface

To ease the design of a confocal reflective system, we developed a freeform surface that consists of a decentered and rotated conic and a plane symmetric polynomial surface.[4,10] To achieve the confocal requirement, the system must use conic surfaces. However, the standard conic surface in current optical design programs is defined having the coordinate system coincident with the pole of the conic. This makes it difficult to design a confocal system because in general the OAR may not intersect the conic pole.

As shown in Fig. 2, the new coordinate system used to describe our freeform surface is tangent with the surface at the intersection of the OAR with the surface. This is quantified by the amount of decenter $y_0$ from the axis of the conic to the origin of the new coordinate system. Further, we add a plane symmetric polynomial to enable the correction of aberrations. This polynomial is described using the coordinates of the new coordinate system, which is centered at the intersection of the OAR with the surface, and is described as

$$z(x, y) = A_1 y^2 + A_2 x^2 y + A_3 y^3 + A_4 x^4 + A_5 x^2 y^2 + A_6 y^4 \ldots.$$

**Table 6** Stop shifting formulas.

| | |
|---|---|
| Uniform astigmatism | $W^*_{02002} = W_{02002}$ |
| Anamorphic distortion | $W^*_{11011} = W_{11011} + 2W_{02002}\overline{S}$ |
| Quadratic piston | $W^*_{20020} = W_{20020} + W_{110011}\overline{S} + W_{02002}\overline{S}^2$ |
| Uniform coma | $W^*_{03001} = W_{03001}$ |
| Linear astigmatism | $W^*_{12101} = W_{12101} + 2W_{03001}\overline{S}$ |
| Field tilt | $W^*_{12010} = W_{12010} + W_{03001}\overline{S}$ |
| Quadratic distortion I | $W^*_{21001} = W_{21001} + W_{12101}\overline{S} + W_{03001}\overline{S}^2$ |
| Quadratic distortion II | $W^*_{21110} = W_{21110} + W_{12101}\overline{S} + 2W_{12010}\overline{S} + 2W_{03001}\overline{S}^2$ |
| Cubic piston | $W^*_{30010} = W_{30010} + W_{21001}\overline{S} + W_{21110}\overline{S} + W_{12101}\overline{S}^2 + W_{12010}\overline{S}^2 + W_{03001}\overline{S}^3$ |

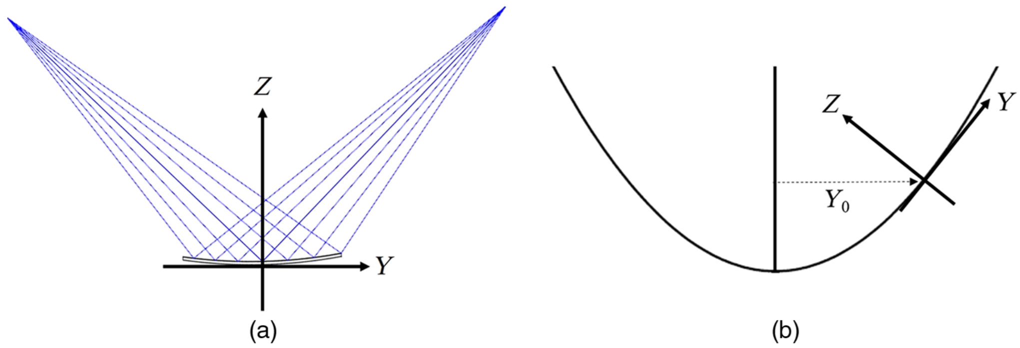


**Fig. 2** (a) An off-axis elliptical surface described about the intersection of the OAR and (b) the decenter $y_0$ is the distance from the conic axis to the origin of the new coordinate system.

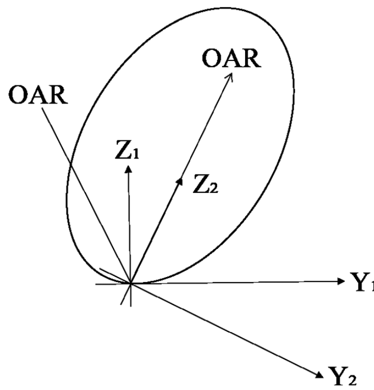


**Fig. 3** Each surface in the system is sandwiched between two coordinate systems and the OAR after reflection coincides with the $z$-axis of the second coordinate system.

As shown in Fig. 3, in actual use the freeform surface is sandwiched between two coordinate systems. The first is tilted by the angle of incidence $I$ of the OAR, and the second is also tilted by the angle $I$ so that the $z$-axis of the second coordinate system coincides with the OAR after reflection on the surface. This procedure simplifies and makes it clear the defining geometry of a confocal system. To define the geometry of such a system all that is required is to specify the OAR angle of incidence $I$ at each freeform surface, the distance to the next surface $t$ along the OAR, the conic decenter $y_0$, the conic constant $k$, the conic vertex radius $r$, and the aspheric coefficients $A_1, A_2, A_3 \dots$ at each surface. If these aspheric terms are not used, then the conic surface is described by its vertex radius, its conic constant, and the decenter $y_0$. However, once a confocal system has been set with the parameters $I$, $r$, $t$, $k$, and $y_0$, then the aspheric terms can be included to allow the control of field aberrations.

One feature of this freeform surface is that the aspheric coefficients of the polynomial directly relate to the aberrations that the freeform surface can introduce. Quadratic aspheric terms influence uniform astigmatism and image anamorphic distortion. Cubic terms influence uniform coma, linear astigmatism and field tilt, and the quadratic distortions. Fourth-order terms influence the primary aberrations of axially symmetric systems.

The fact that the surfaces of confocal systems are off-axis conics, or off-axis Cartesian ovoids for refractive systems, leads to some simplification in their optical testing given that the surfaces have two foci. The presence of the additional polynomial terms will result in that the foci will have aberration. This aberration might be compensated with a null corrector, diffractive, or refractive.

## 6 Linear Astigmatism and Field Tilt

Within fourth-order aberration theory and in a confocal of the image mirror system, linear astigmatism is proportional to field tilt;[1] they vanish simultaneously. Linear astigmatism is given as

$$W_{12101} = Ж \sum_{i=1}^{k} \left[ \sin(I) \frac{y}{r} \right]_i ,$$

where Ж is the system Lagrange invariant, $y$ is the first-order marginal ray height, $r$ is the surface radius of curvature, $I$ is the OAR angle of incidence in the surface, and $k$ is the number of surfaces in the system. Thus, under small OAR angles of incidence a condition for the absence of linear astigmatism and field tilt is

$$0 = \sum_{i=1}^{k} \left[ \sin(I) \frac{y}{r} \right]_i .$$

Field tilt is the tilt of the sagittal field curve at the OAR. For a confocal refractive system, the condition for the absence of linear astigmatism becomes

$$0 = \sum_{i=1}^{k} \left[ n \sin(I) \Delta\left( \frac{u}{n} \right) \right]_i .$$

We now discuss a real ray-based condition for the absence of linear astigmatism. As shown in Table 3, in a confocal mirror system pupil quadratic distortion I equals image field tilt, $\overline{W}_{21001} = W_{12010}$. Pupil quadratic distortion II equals linear astigmatism, $\overline{W}_{21110} = W_{12101}$. Quadratic distortion I is known as smile distortion in spectroscopic instruments because the image of the slit is curved. Quadratic distortion II represents keystone distortion. There is no anamorphic distortion of the pupil, or of the image, in a confocal mirror system.

Let us assume that the stop aperture coincides with the entrance pupil in object space and that the stop aperture is circular and perpendicular to the OAR. In addition, the object plane is also perpendicular to the OAR. In this case, the optical flux $\phi$ accepted by a confocal system is

$$\phi = \pi L_0 dx\, dy\, \sin(U_x) \sin(U_y),$$

where $L_0$ is the radiance of the object, $dx$ and $dy$ are the width and height of the object, and $U_x$ and $U_y$ are the angles with respect to the OAR of real marginal rays defined by $\vec{i} \cdot \vec{\rho} = 1$ and $\vec{i} \cdot \vec{\rho} = 0$, in the plane of symmetry and perpendicularly to it (in object space $U_x = U_y$). The optical power $\phi'$ that passes through an area defined by the first-order image of width and height $dx'$ and $dy'$ is

$$\phi' = \frac{\pi}{2} L_0 dx'\, dy'\, \sin(U'_x)[\sin(U'_{+y}) - \sin(U'_{-y})],$$

where $U'_{+y}$, $U'_{-y}$, and $U'_x$ are the angles with respect to the optical axis in image space of the marginal rays defined by $\vec{i} \cdot \vec{\rho} = 1$, $\vec{i} \cdot \vec{\rho} = -1$, and $\vec{i} \cdot \vec{\rho} = 0$.

If the optical flux accepted by the entrance pupil must pass through the area defined by the first-order image, then we must have

$$dx'\, \sin(U'_x) = dx\, \sin(U_x) \quad \text{and}$$
$$dy'[\sin(U'_{+y}) - \sin(U'_{-y})] = 2dy\, \sin(U_y).$$

The relationship $dx'\, \sin(U'_x) = dx\, \sin(U_x)$ is the sine condition and makes the system free from linear coma. The relationship $dy'[\sin(U'_{+y}) - \sin(U'_{-y})] = 2dy\, \sin(U_y)$ is satisfied to second-order in the aperture if

$$\sin(U'_{+y}) = -\sin(U'_{-y}).$$

This condition makes the on-axis beam symmetrical with respect to the OAR. Alternatively, the on-axis beam is symmetrical in the plane of symmetry if the sum of the pupil keystone and pupil smile distortion is zero:

$$\bar{W}_{21001}(\vec{i} \cdot \vec{H})(\vec{\rho} \cdot \vec{\rho}) + \bar{W}_{21110}(\vec{i} \cdot \vec{\rho})(\vec{H} \cdot \vec{\rho}) = 0.$$

Given the equality between the distortion terms and field tilt and linear astigmatism:

$$\overline{W}_{21001}(\vec{i} \cdot \vec{H})(\vec{\rho} \cdot \vec{\rho}) = W_{12010}(\vec{i} \cdot \vec{H})(\vec{\rho} \cdot \vec{\rho}),$$

$$\overline{W}_{21110}(\vec{i} \cdot \vec{\rho})(\vec{H} \cdot \vec{\rho}) = W_{12101}(\vec{i} \cdot \vec{\rho})(\vec{H} \cdot \vec{\rho}),$$

and as the sum of field tilt and linear astigmatism is the tilt of the tangential field curve at the optical axis, it results in that

$$\sin(U'_{+y}) = -\sin(U'_{-y}),$$

is a condition for zero tilt of the tangential field curve. To determine this condition, only two real marginal rays are required to be traced from the on-axis field point and in the plane of symmetry. This condition was tested with several two-, three-, and four-mirror confocal systems; field tilt was also corrected in consistency with fourth-order theory.[1]

In a confocal system, linear astigmatism and field tilt do not depend on the stop location. Therefore, stop shifting can be performed to locate the stop aperture to meet first-order requirements or to further improve the image quality.

In the general plane symmetric mirror system and according to Table 3, the absence of linear astigmatism implies the absence of pupil keystone distortion as seen from the image plane and the absence of field tilt implies the absence of pupil smile distortion as seen from the image plane. Consequently, three marginal rays defined by $\vec{i} \cdot \vec{\rho} = 1$, $\vec{i} \cdot \vec{\rho} = -1$, and $\vec{i} \cdot \vec{\rho} = 0$ can be traced to a plane perpendicular to the OAR in image space located at the exit pupil point in the OAR. This may not be the exit pupil plane as this can be tilted. The stop is assumed to be in object space and perpendicular to the OAR. If $Y^+$ and $Y^-$ are the ray heights at that plane for the rays $\vec{i} \cdot \vec{\rho} = 1$ and $\vec{i} \cdot \vec{\rho} = -1$, and if $\Delta Y$ is the ray coordinate in the direction of $\vec{i}$ for the ray $\vec{i} \cdot \vec{\rho} = 0$, then the absence of keystone and smile distortion requires $Y^+ = -Y^-$ and $\Delta Y = 0$. The condition $Y^+ = -Y^-$ is equivalent to the condition $\sin(U'_{+y}) = -\sin(U'_{-y})$. A practical matter is that only rays from the on-axis field point are needed to correct for linear astigmatism and field tilt. These conditions were verified in some four-mirror plane symmetric systems that were not confocal.

## 7 Design Examples

In this section, designs examples are presented that illustrate how the method is implemented. The freeform surface was programmed as a user-defined surface[10] in Zemax OpticsStudio. Other design examples have been previously reported.[3,4]

### 7.1 *Two-Mirror System Confocal of the Object and Image*

The first example is a two-mirror objective with an object at infinity. To achieve confocal imaging along the OAR, the first mirror is an off-axis parabola as shown in Fig. 4 and the second mirror is a hyperbola as shown in Fig. 5. The angle of incidence of the OAR in each mirror is 22.5 deg so that the OAR makes a 90 deg turn. The stop aperture is at the primary mirror.

To correct for field tilt $W_{12010}(\vec{i} \cdot \vec{H})(\vec{\rho} \cdot \vec{\rho})$ and linear astigmatism $W_{12101}(\vec{i} \cdot \vec{\rho})(\vec{H} \cdot \vec{\rho})$, the vertex radius of curvature of the secondary mirror was used as an effective

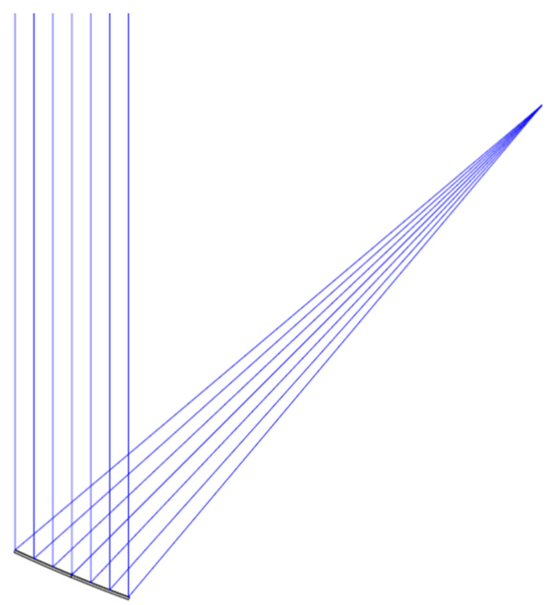

**Fig. 4** Primary mirror is an off-axis parabola.

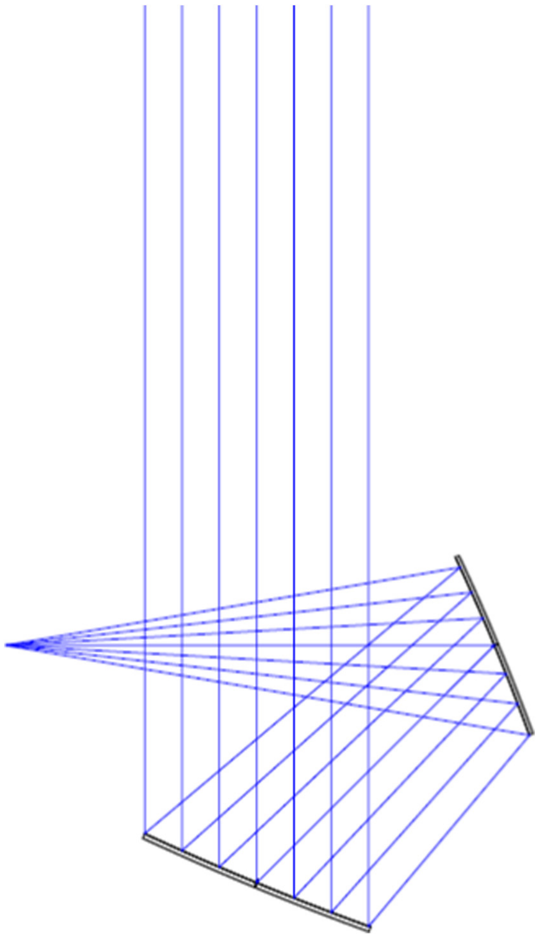

**Fig. 5** Secondary mirror is a hyperbola.

degree of freedom. Then to correct for linear coma $W_{13100}(\vec{H}\cdot\vec{\rho})(\vec{\rho}\cdot\vec{\rho})$ third-, fourth-, fifth-, and sixth-order terms in the freeform polynomial description $z(x,y)$ of the surfaces were released as design variables. After optimization, the design is limited by field curvature $W_{22000}(\vec{H}\cdot\vec{H})(\vec{\rho}\cdot\vec{\rho})$ and quadratic astigmatism $W_{22200}(\vec{H}\cdot\vec{\rho})^2$. However, the performance is near diffraction limited in the visible over a 2 deg field of view at $F/3$ and at an aperture of 50 mm. The maximum distortion aberration is 0.27% over the 2 deg field of view. The final design is shown in Fig. 6. Note that the use of the aspheric coefficients $A_i$ does not change the system layout, or second-order system properties, given that the aspheric polynomial $z(x,y) = A_1y^2 + A_2x^2y + A_3y^3 + A_4x^4 + A_5x^2y^2 + A_6y^4\ldots$ is defined about the intersection of the OAR with the surface.

### 7.2 *Two-Mirror System Confocal of the Pupils*

The second example is also a two-mirror system with the object at infinity. However, the stop aperture is in front of the primary mirror and therefore to achieve the confocal requirement of the pupil the primary mirror is elliptical in shape as shown in Fig. 7. The secondary mirror is hyperbolic as shown in Fig. 8. Both, Figs. 7 and 8 show that the stop is imaged stigmatically along the OAR.

Figure 9 shows the two mirror system with rays from the object at infinity. To correct for uniform coma

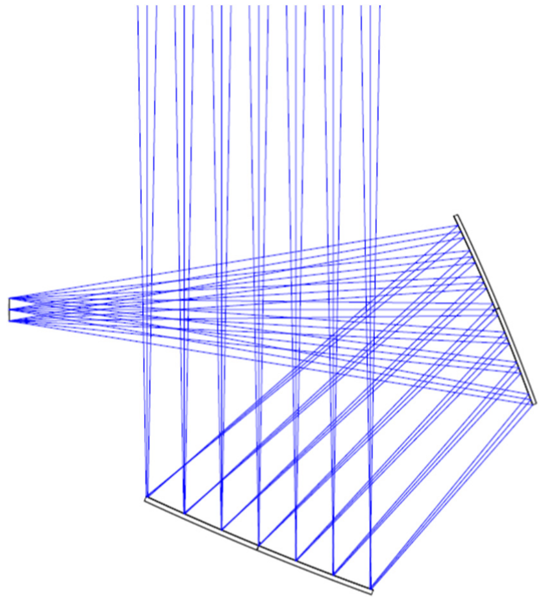

**Fig. 6** Two-mirror design working over a 2-deg field of view at $F/3$.

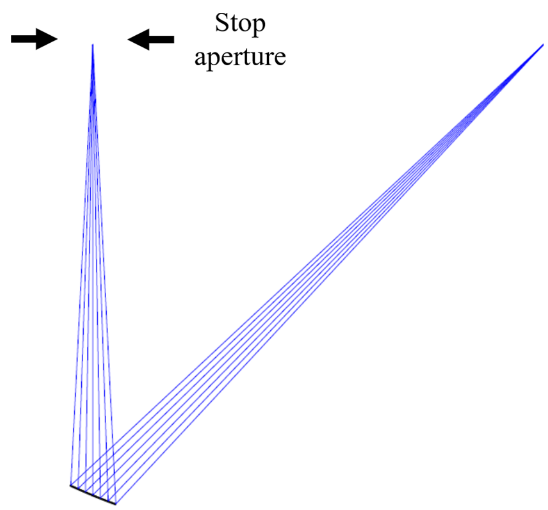


**Fig. 7** Primary mirror is elliptical.

$W_{03001}(\vec{i}\cdot\vec{\rho})(\vec{\rho}\cdot\vec{\rho})$, the vertex radius of curvature of the secondary mirror was used as an effective degree of freedom. It is worth emphasizing that because the system is confocal of the pupils there is no uniform, linear, or quadratic astigmatism present in the system.

The system as shown in Fig. 10 suffers from about 4.86 deg of field tilt aberration. Residual high-order aberrations were corrected using the polynomial terms in the freeform surface description. The performance is comparable to the first example, except that the stop is remote and the $F$-number is lower at $F/2.7$. Stop shifting can be performed to locate the stop at a desired position. The maximum distortion aberration is also 0.27% over the 2 deg field of view.

## 8 Design Method Step by Step

Table 1 shows the primary aberrations of a plane symmetric system. These aberrations are divided into three subgroups

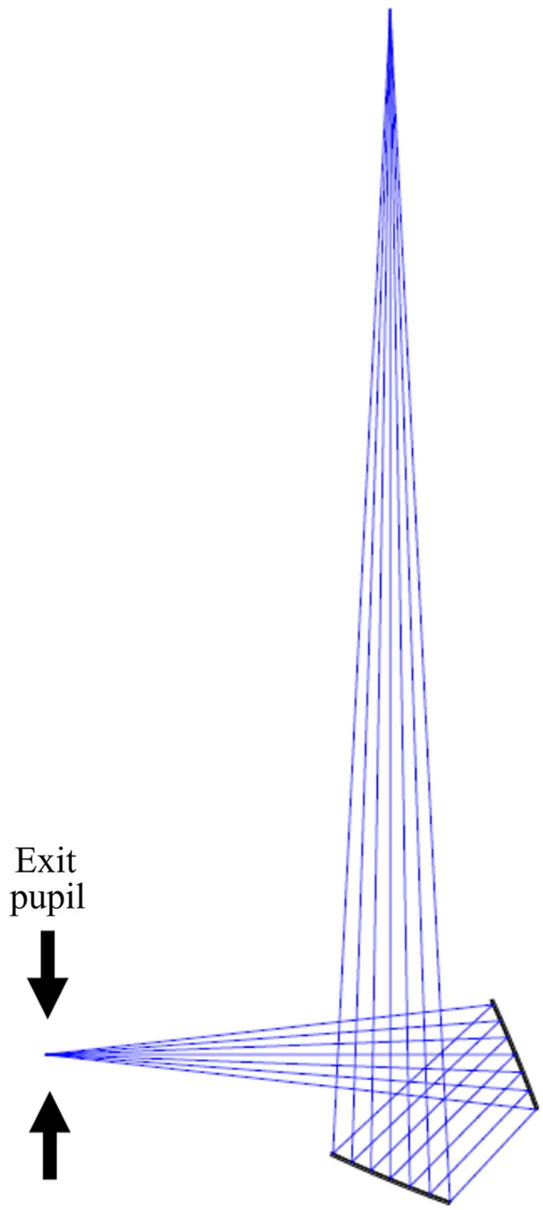


**Fig. 8.** Secondary mirror is hyperbolic.

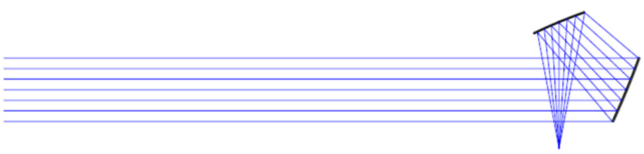

**Fig. 9** The two-mirror system with the object at infinity.

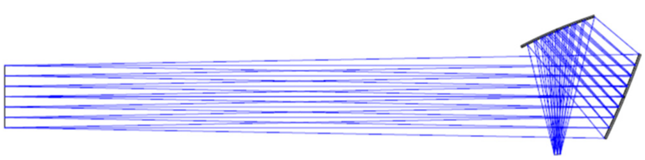

**Fig. 10** The two-mirror system with the object at infinity covering a field of view of 2 deg. Note that the stop aperture is remote and in front of the primary mirror.

that have (1) an infinity number of planes of symmetry (axial symmetry), (2) two planes of symmetry, and (3) one plane of symmetry. Accordingly, a first step to design a confocal system is to identify an axially symmetric system that has its primary aberrations corrected. The second step is to convert the system into an axially symmetric system that is confocal of the image. In this step, all radii of curvature and surface thickness are maintained, and all surface aspheric coefficients are changed to satisfy the confocal requirement. The third step is to tilt the system surfaces while maintaining the confocal condition to achieve a configuration that meets packaging requirements and that is free from linear astigmatism. The fourth step is to optimize the system for image quality using only the polynomial aspheric coefficients and the distance to the image plane as optimization variables.

## 9 TMA Design Examples

Three-mirror anastigmatic systems (TMAs)[11,12] are an important class of mirror systems. Originally, TMAs have been designed as off-axis sections of axially symmetric systems. The design of three TMAs using freeform surfaces is illustrated in this section.

**Example 1**

The starting point for this design example is an axially symmetric, there-mirror flat-field, and anastigmatic system as shown in Fig. 11(a). The radii of curvature and mirror conic constants are used to correct for aberrations. Figure 11(b) shows the system, made unobscured by tilting the mirrors while maintaining the confocal requirement. Linear astigmatism and field tilt have been corrected by requiring $Y^+ = -Y^-$ and $\Delta Y = 0$. Figure 11(c) shows the design optimized using only the polynomial terms on each mirror and the distance to the image plane as variables. Table 7 shows its constructional data. Note that the system description is minimal in data and simple as it easily conveys the system geometry. The off-axis conic and polynomial surface is provided for Zemax OpticStudio lens design software as a user-defined surface at Ref. 10.

Figure 12 shows beam footprints at a plane perpendicular to the OAR and located at the exit pupil, for the on-axis beam, and for three full-field positions. Note the absence of keystone and smile distortion in the on-axis beam footprint in consistency with the absence of field tilt and linear astigmatism. The extreme rays for the on-axis beam are indicated by $\vec{i} \cdot \vec{\rho} = 1$, $\vec{i} \cdot \vec{\rho} = -1$, and $\vec{i} \cdot \vec{\rho} = 0$.

**Example 2**

Of interest is the design of mirror systems that have an external stop, an intermediate image, or an external exit pupil. The following design example offers these three features and it is based on the design of Ref. 12. However, given the use of freeform surfaces, and the flexibility to not maintain axial symmetry, it was possible to have access to the intermediate image, and to obtain good image quality without the need of a correcting fourth mirror. The design starts with a two-mirror anastigmatic system that uses spherical surfaces as shown in Fig. 13(a). This design has a virtual image and has field curvature; the primary is concave and the secondary is convex. By adding a concave reimaging tertiary mirror as shown in Fig. 13(b), a real image is obtained and Petzval field curvature is corrected. Further, using the conic constants of the primary and secondary

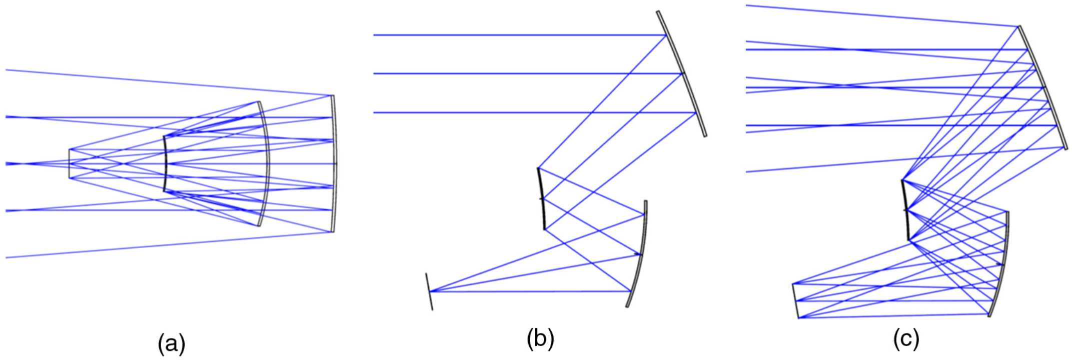


**Fig. 11** (a) An axially symmetric, three-mirror, flat-field and anastigmatic system. (b) The TMA has been made unobscured and converted into a confocal system free from field tilt and linear astigmatism. (c) Only the polynomial terms and the distance to the image have been used to minimize the system aberrations in a circular field of view of $+/-4.5$ deg.

**Table 7** Prescription for flat-field, three-mirror anastigmat, $F/2.66$; $f = 36.26$ mm; FOV $= +/-4.5$ deg, thickness is along the OAR, $I$ is the angle of incidence of the OAR.

| Surface | Radius | Thickness | Conic constant | Off-axis $Y_0$ | $I$ |
|---|---|---|---|---|---|
| 1 | −150 | −30 | −1.0 | 57.3315 | −21 deg |
| 2 (STOP) | −30.3191 | 18 | −0.3647 | −36.4368 | 36 deg |
| 3 | −38 | −34.3884 | −0.1727 | 33.2803 | −20 deg |
| | | | Aspheric coefficients | | |
| | | | $A_2$, $A_3$, $A_4$, $A_5$, $A_6$ | | |
| | $X^2Y$ | $Y^3$ | $X^4$ | $X^2Y^2$ | $Y^4$ |
| 1 | $3.2559 \times 10^{-6}$ | $-4.231 \times 10^{-6}$ | $2.8549 \times 10^{-7}$ | $2.7887 \times 10^{-7}$ | $1.7113 \times 10^{-7}$ |
| 2 | $3.0021 \times 10^{-5}$ | $-2.929 \times 10^{-5}$ | $-9.591 \times 10^{-7}$ | $-4.682 \times 10^{-6}$ | $-8.425 \times 10^{-7}$ |
| 3 | $6.7614 \times 10^{-6}$ | $-7.34 \times 10^{-6}$ | $-5.368 \times 10^{-7}$ | $-1.637 \times 10^{-6}$ | $-4.955 \times 10^{-7}$ |

mirrors, the system can be maintained as anastigmatic. Thus, except for distortion, we have an axially symmetric system corrected for its primary aberrations. For clarity, Figs. 13(a) and 13(b) have been drawn with a single off-axis beam at large field. The next step is to tilt the mirrors to make the system unobscured, and to make the system confocal of the image as shown in Fig. 13(c). Field tilt and linear astigmatism have been corrected by requiring $Y^+ = -Y^-$, and $\Delta Y = 0$.

The next step is to minimize the remaining aberrations using only the coefficients $A_1, A_2, A_3 \ldots$ at each surface. The prescription of this TMA system is given in Table 8, and the RMS spot size versus the field of view is given in Table 9 for a system with a focal length of 96.5 mm and for two cases. The first case is using up to fourth-order aspheric coefficients in the surfaces. The second case is using up to sixth-order aspheric coefficients. The maximum distortion for each case is also given. Depending on the field of view, optical speed, image plane tilt, distortion, and image quality, many design trade-offs can be made. Figure 13(d) shows one way in which the system can be folded with a flat mirror to improve packaging.

### Example 3

In designing a TMA such as that of the previous example, there is the option to tilt the secondary mirror in the opposite direction as shown in Fig. 14. This system is confocal of the image but is not corrected for field tilt and linear astigmatism. Such a correction would require decreasing the tilt of the tertiary mirror, and then the focusing light beams would fall on the secondary mirror making the system impractical. However, the residual field tilt and linear astigmatism of the system in Fig. 14 are not too large.

Let us consider now a rotation $\phi_2$ of the secondary mirror in Fig. 14 around the OAR before it reflects on the secondary mirror. This rotation would break the plane symmetry of the system but will maintain the confocal condition. Similarly, the tertiary mirror can be rotated an angle $\phi_3$ about the OAR further breaking the plane symmetry, but likewise, the confocal condition of perfect imaging along the OAR, surface after surface, would be maintained. The result is a confocal system built up with plane symmetric surfaces but that does not have an identifiable symmetry. Then we have two more degrees of freedom, $\phi_2$ and $\phi_3$, to mitigate aberration, in particular field tilt and linear astigmatism.

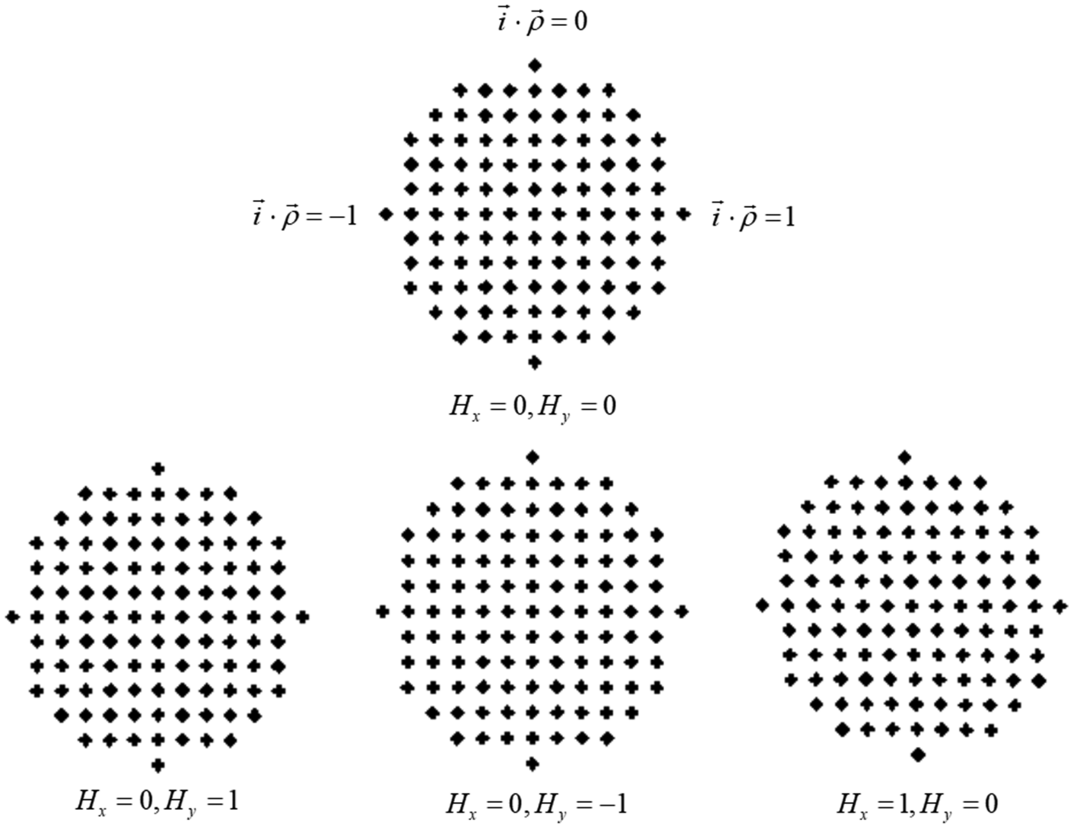


**Fig. 12** Beam footprints for the on-axis beam and three fullfield positions. The on-axis beam footprint does not have keystone or smile distortion in consistency with the absence of field tilt and linear astigmatism.

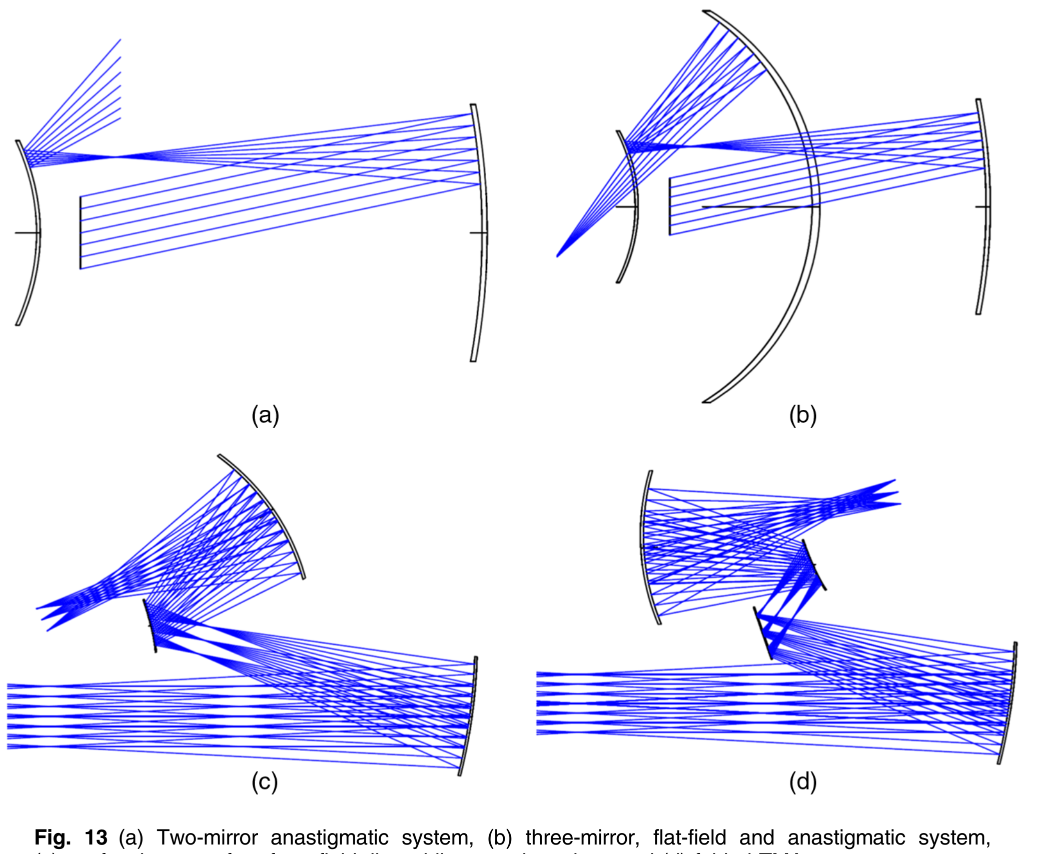


**Fig. 13** (a) Two-mirror anastigmatic system, (b) three-mirror, flat-field and anastigmatic system, (c) confocal system free from field tilt and linear astigmatism, and (d) folded TMA system.

**Table 8** Prescription for flat-field, three-mirror anastigmat with external stop, intermediate image, and external exit pupil. $F/4$; $f = 3.8$; FOV $= 6$ deg $\times$ 8 deg, thickness is along the OAR, $I$ is the angle of incidence of the OAR. The stop aperture is at a distance of seven units in front of the primary mirror.

| Surface | Radius | Thickness | Conic constant | Off-axis $Y_0$ | $I$ (deg) |
|---|---|---|---|---|---|
| 1 | −9.0 | −5.5 | −1.0 | −1.264867 | 8 |
| 2 | −2.591215 | 2.75 | −17.4724 | 0.357903 | −30 |
| 3 | −3.638902 | −4.239 | −0.03889 | 3.000175 | 9.2357 |

Aspheric coefficients

$A_2$, $A_3$, $A_4$, $A_5$, $A_6$

| | $X^2Y$ | $Y^3$ | $X^4$ | $X^2Y^2$ | $Y^4$ |
|---|---|---|---|---|---|
| 1 | $-5.115\times10^{-5}$ | −3.930E − 5 | $1.241\times10^{-4}$ | $3.273\times10^{-4}$ | $1.238\times10^{-4}$ |
| 2 | $8.642\times10^{-3}$ | $8.659\times10^{-3}$ | $-2.582\times10^{-2}$ | $-1.213\times10^{-2}$ | $-2.005\times10^{-2}$ |
| 3 | $8.4116\times10^{-5}$ | $4.921\times10^{-5}$ | $2.280\times10^{-4}$ | $6.349\times10^{-4}$ | $1.902\times10^{-4}$ |

**Table 9** TMA RMS spot size in $\mu$m versus field of view $X$ deg, $Y$ deg. $f = 96.5$ mm (the system has been scaled up).

| | 0 deg, 0 deg | 0 deg, 3 deg | 0 deg, −3 deg | 4 deg, 0 deg | 4 deg, 3 deg | 4 deg, −3 deg | Distortion (%) |
|---|---|---|---|---|---|---|---|
| RMS | 11 | 15 | 13 | 14 | 20 | 13 | 6.7 |
| RMS | 8 | 5 | 7 | 10 | 8 | 5 | 2.6 |

When the system of Fig. 14 is optimized using the rotations $\phi_2$ and $\phi_3$ and the aspheric coefficients $A_1, A_2, A_3 \ldots$ at each surface, the image quality is acceptable as shown with RMS spot size versus the field of view in Table 10. The optimized mirror system is shown in Fig. 15 and its prescription is given in Table 11. Thus, a confocal system can depart from plane symmetry to gain further design flexibility. The theory of aberrations of a combination of plane symmetric systems is found in Ref. 13.

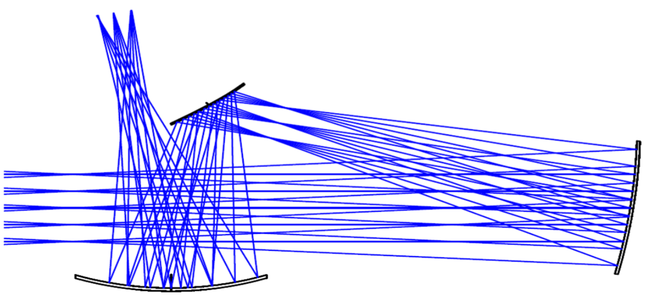

**Fig. 14** Confocal of the image three-mirror system.

To rotate the secondary mirror, a third coordinate system is set right after the second coordinate system of the first mirror. When the secondary mirror rotates about the OAR, the tertiary mirror also changes position as it is coupled to

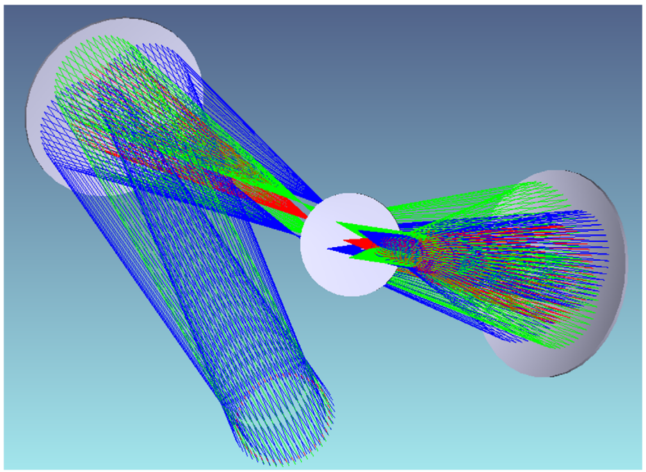

**Fig. 15** TMA system using plane symmetric mirrors but having no identifiable symmetry.

**Table 10** TMA RMS spot size in $\mu$m versus field of view $X$ deg, $Y$ deg. $f = 101$ mm (the system has been scaled up).

| | 0 deg, 0 deg | 0 deg, 3 deg | 0 deg, −3 deg | 3 deg, 0 deg | −3 deg, 0 deg | Distortion (%) |
|---|---|---|---|---|---|---|
| RMS | 2.4 | 5.2 | 4.6 | 3.7 | 5.7 | 4.6 |

**Table 11** Prescription for flat-field, three-mirror anastigmat with external stop, intermediate image, and external exit pupil, lacking plane symmetry. $F/4$; $f = 3.9$; FOV $= 6$ deg $\times$ 6 deg, thickness is along the OAR, $I$ is the angle of incidence of the OAR, and $\phi$ is the angle of rotation about the OAR. The stop aperture is at a distance of seven units in front of the primary mirror.

| Surface | Radius | Thickness | Conic constant | Off-axis $Y_0$ | $I$ (deg) | $\phi$ (deg) |
|---|---|---|---|---|---|---|
| 1 | −9.0 | −5.5 | −1.0 | −1.264867 | 8 | |
| 2 | −2.591215 | 2.75 | −21.3337 | −0.505134 | 42 | 134.646 |
| 3 | −3.638902 | −4.176 | −0.04014 | −3.202241 | -10 | 12.399 |

Aspheric coefficients

$A_2, A_3, A_4, A_5, A_6, A_7, A_8, A_9, A_{10}, A_{11}, A_{12}, A_{13}$

| | $X^2Y$ | $Y^3$ | $X^4$ | $X^2Y^2$ | $Y^4$ | $X^4Y$ |
|---|---|---|---|---|---|---|
| 1 | $-3.01\times10^{-5}$ | $4.6137\times10^{-5}$ | $-9.757\times10^{-5}$ | $-1.976\times10^{-4}$ | $-6.692\times10^{-5}$ | $1.414\times10^{-4}$ |
| 2 | $4.167\times10^{-3}$ | $-2.78\times10^{-3}$ | −0.0844 | −0.1282 | −0.01485 | −0.2571 |
| 3 | $6.567\times10^{-5}$ | $-7.748\times10^{-5}$ | $-3.647\times10^{-5}$ | $-5.256\times10^{-5}$ | $3.524\times10^{-5}$ | $-1.931\times10^{-4}$ |
| | $X^2Y^3$ | $Y^5$ | $X^6$ | $X^4Y^2$ | $X^2Y^4$ | $Y^6$ |
| 1 | $-1.168\times10^{-5}$ | $-4.216\times10^{-5}$ | $3.608\times10^{-5}$ | $5.568\times10^{-5}$ | $-5.015\times10^{-5}$ | $2.1682\times10^{-5}$ |
| 2 | −0.1644 | −0.04297 | 0.10305 | −0.0206 | $-9.603\times10^{-3}$ | −0.07574 |
| 3 | $-1.371\times10^{-4}$ | $4.294\times10^{-5}$ | $2.406\times10^{-5}$ | $1.585\times10^{-4}$ | $5.4735\times10^{-5}$ | $-4.342\times10^{-5}$ |

the secondary mirror. To rotate the tertiary mirror, a third coordinate system is set right after the second coordinate system of the secondary mirror. The rotation is about the $z$-axis of the third coordinate system, which coincides with the OAR. Thus by rotating the mirrors of a confocal system about the OAR, a dimension of design possibilities is opened. This method of rotating surfaces is simple to implement in lens design software.

Of concern in the design of systems that use freeform surfaces is their departure from the base conic surface. This can be first evaluated by removing the aspheric coefficients of one surface and analyzing the residual aberration. If this aberration is a few waves, then the surface might be within the reach of testing of an interferometer. If the aspheric terms represent a significant departure from the base conic surface, then one can try to release as variables the radius, conic constant, and decenter $y_0$ of the surface, and optimize to reduce the aspheric deformation coefficients $A_1, A_2, A_3 \ldots$

## 10 Conclusion

This paper reviews the aberrations of confocal reflective systems and advances their theory. Such systems may not only be confocal of the object and image but can be confocal of the pupils. We provide the aberrations of a system that is confocal of the pupils and show that they are simplified. In addition, we provide stop shifting formulas for the aberrations of a plane symmetric system. Five design examples are presented that illustrate how the design of confocal systems can be carried out. Of practical use is the real ray conditions presented for the absence of linear astigmatism and field tilt. These require the trace of three real rays from the on-axis field point. The design method outlined is powerful and simple to implement enabling an optical engineer to design unobscured reflective systems in a systematic manner.

## References


1. J. Sasian, "How to approach the design of a bilateral symmetric optical system," *Opt. Eng.* **33**(6), 2045–2061 (1994).
2. J. Sasian, "Review of methods for the design of unsymmetrical optical systems," *Proc. SPIE* **1396**, 463–466 (1990).
3. J. Sasian, "Optical design of reflective wide-field cameras," *Proc. SPIE* **7060**, 70600C (2008).
4. D. Reshidko and J. Sasian, "A method for the design of unsymmetrical optical systems using freeform surfaces," *Proc. SPIE* **10590**, 105900V (2017).
5. J. C. Papa, J. M. Howard, and J. P. Rolland, "Starting point designs for freeform four-mirror systems," *Proc. SPIE* **10590**, 105900Z (2017).
6. S. Chang, "Compact wide-field off-axis two-mirror system with field corrector," *Proc. SPIE* **9948**, 99481B (2016).
7. J. Sasian, "The method of confocal mirror design," *Proc. SPIE* **10690**, 1069015 (2018).
8. J. Sasian, "Pupil aberrations in tilted component systems that are plane symmetric," in *International Optical Design, Technical Digest (CD)*, Optical Society of America, paper MC2 (2006).
9. K. O'shea, "Lens design approach to optical relays," MSc Thesis, University of Arizona (2005).
10. D. Reshidko and J. Sasian, "User defined freeform surface," https://wp.optics.arizona.edu/jsasian/wpcontent/uploads/sites/33/2017/07/Surface.zip (2017).
11. W. B. Wetherell and D. A. Womble, "All-reflective three element objective," US Patent 4,240,707 (1980).
12. L. G. Cook, "Off-axis three-mirror anastigmatic having corrector mirror," US Patent 5,550,672 (1996).
13. L. B. Moore, A. M. Hvisc, and J. Sasian, "Aberration fields of a combination of plane symmetric systems," *Opt. Express* **16**, 15655–15670 (2008).


**José Sasián** is a professor at the College of Optical Sciences at the University of Arizona. His research interests are in optical engineering, education in optics, art in optics and optics in art, optical design, lithography, opto-mechanics, optical testing and fabrication, light in gemstones, and light propagation.